arXiv:1008.0298v3 [physics.bio-ph] 26 Jan 2011

Distribution of dwell times of a ribosome: effects of infidelity, kinetic proofreading and ribosome crowding

Ajeet K. Sharma[1] and Debashish Chowdhury*[1]

[1] *Department of Physics, Indian Institute of Technology, Kanpur 208016, India.*

Ribosome is a molecular machine that polymerizes a protein where the sequence of the amino acid residues, the monomers of the protein, is dictated by the sequence of codons (triplets of nucleotides) on a messenger RNA (mRNA) that serves as the template. The ribosome is a molecular motor that utilizes the template mRNA strand also as the track. Thus, in each step the ribosome moves forward by one codon and, simultaneously, elongates the protein by one amino acid. We present a theoretical model that captures most of the main steps in the mechano-chemical cycle of a ribosome. The stochastic movement of the ribosome consists of an alternating sequence of pause and translocation; the sum of the durations of a pause and the following translocation is the time of dwell of the ribosome at the corresponding codon. We derive the analytical expression for the distribution of the dwell times of a ribosome in our model. Whereever experimental data are available, our theoretical predictions are consistent with those results. We suggest appropriate experiments to test the new predictions of our model, particularly, the effects of the quality control mechanism of the ribosome and that of their crowding on the mRNA track.

PACS numbers: 87.16.ad, 87.16.Nn, 87.10.Mn

I. INTRODUCTION

The primary structure of a protein consists of a sequence of amino acid residues linked together by peptide bonds. Therefore, a protein is also referred to as a polypeptide which is essentially a linear hetero-polymer, the amino acid residues being the corresponding monomers. The sequence of the amino acid residues in a polypeptide is dictated by that of the codons, each of which is a triplet of nucleotides, on a messenger RNA (mRNA) that serves as the template for the polypeptide. The actual polymerization of each protein from the corresponding mRNA template is carried out by a macromolecular machine called ribosome [1–3] and the process is referred to as *translation* (of genetic code). The polymerization of protein takes places in three stages that are identified as *initiation*, *elongation* (of the protein) and *termination*.

The ribosome also utilizes the template mRNA as a track for its own movement; it steps forward by one codon at a time while, simultaneously, it elongates the growing polypeptide by one amino acid monomer. Therefore, ribosome is also regarded as a motor that, like other molecular motors, takes input (free-) energy from the hydrolysis of a nucleotide tri-phosphate to move along a filamenous track [4]. In fact, a ribosome hydrolyzes two molecules of Guanosine tri-phosphate (GTP) to move forward by one codon.

Enormous progress has been made in the last decade in the fundamental understanding of the structure, energetics and kinetics of ribosomes [5–14]. Recent single molecule studies of ribosomes [15–21] has thrown light on its operational mechanism.

In single molecule experiments, it has been observed that a ribosome steps forward in a stochastic manner; its stepping is characterized by an alternating sequence of pause and translocation. The sum of the durations of a pause and the following translocation defines the time of a dwell of the ribosome at the corresponding codon. The time of dwell of a ribosome varies randomly from one codon to another. This randomness arises from two different sources: (i) *intrinsic* fluctuations associated with the Brownian forces as well as the low of concentrations of the molecular species involved in the chemical reactions, and (ii) *extrinsic* fluctuations caused by the inhomogeneities of the sequence of nucleotides on the template mRNA [22]. Because of the sequence inhomogeneity of the mRNA templates used by Wen et al. [23], the dwell time distribution (DTD) measured in their single-molecule experiment reflects a combined effect of the intrinsic and extrinsic fluctuations on the dwell time. In contrast, in this paper we focus on situations (to be explained in detail in the following sections) where the randomness of the dwell times arises exclusively from *intrinsic* fluctuations.

The probability density $f(t)$ of the dwell times of a ribosome, measured in single-molecule experiments [23], has been compared with the corresponding data obatined from computer simulations [24]. It has been claimed that the data do not fit a single exponential thereby indicating the existence of more than one rate-limiting step in the

* Corresponding author(E-mail: debch@iitk.ac.in)

mechano-chemical cycle of each ribosome. In fact, the best fit to the simulation data was achieved with five different rate-determining steps [24].

A systematic analytical derivation of the DTD of the ribosomes was presented recently [25] from a kinetic theory of translation [26] that also involves essentially five steps in the mechano-chemical cycle of a ribosome. However, the model developed in ref.[26] ignores some of the key features of the mechano-chemical cycle of an individual ribosome during the elongation stage. For example, a ribosome deploys an elaborate proofreading mechanism to select the correct amino acid dictated by the template (and to reject the incorrect ones) to ensure high translational fidelity. Nevertheless, occasionally, translational errors take place. In this paper we extend Basu and Chowdhury's original model [26] by capturing the processes of proofreading and allowing for the possibility of imperfect fidelity of translation. Moreover, the identification of the mechano-chemical states as well as the nature of the transitions among these states is revised in the light of the empirical facts established in the last couple of years. Using this revised and extended kinetic model of translation [27], we *analytically* calculate the probability density $f(t)$ of the dwell times of ribosomes.

The DTD derived in this paper is qualitatively similar to that observed by Wen et al. in their single molecule experiments [23]. However, because of the sequence inhomogeneity of the template mRNA used in the experiment of Wen et al.[23], their data cannot be compared quantitatively with our analytical expression for $f(t)$. Therefore, we propose a concrete experimental set up required for a quantitative testing of our theoretical predictions. However, till such experiments are actually carried out, the results reported here will continue to provide insight into the mechanistic origin of the qualitative features of the DTD. Moreover, attempts are being made to extend our model to capture sequence inhomogeneities of mRNAs and to calculate the corresponding DTDs of ribosomes *analytically*.

Interestingly, the inverse of the mean dwell time is the average velocity V of the ribosome motor. Since, in our model, the ribosome is not allowed to back track on the mRNA template, V is also the mean rate of elongation of the polypeptide. We show that V satisfies an equation that resembles the Michaelis-Menten equation for the average rate of simple enzymatic reactions [28].

It is well known that most often a large number of ribosomes simultaneously move on the same mRNA track each polymerizing one copy of the same protein. This phenomenon is usually referred to as ribosome traffic because of its superficial similarity with vehicular traffic on highways [26, 29–41] In this paper we also report the effect of steric interactions of the ribosomes in ribosome traffic on their DTD.

II. THE MODEL

We develope here a theoretical model for the polymerization of a protein by ribosomes using an artificially synthesized mRNA template that consists of a *homogeneous* sequence (i.e., all the codons of which are identical). In the surrounding medium, *two* species of amino-acids are available only one of which is the correct one according to the genetic code. The ribosome deploys a quality control system that rejects the amino acid monomer if it is incorrect. If this quality control system never fails, perfect fidelity of translation would result in a homopolymer whose constituent amino acid monomers are all identical. However, occasionally, wrong amino acid monomer escapes the quality control system. Such translational errors, whereby a wrong amino acid monomer is incorporated in the elongating protein, results in a *hetero-polymer*. We'll study the effects of the quality control system on the DTD of the ribosomes.

A ribosome consists of two interconnected subunits which are designated as "large" and "small" (see fig.1). The small subunit binds with the mRNA track and decodes the genetic message of the codon whereas the polymerization of the protein takes place in the large subunit. The operations of the two subunits are coordinated by a class of adapter molecules, called tRNA (see fig.1). One end of a tRNA helps in the decoding process by matching its anti-codon with the codon on the mRNA while its other end carries an amino acid; in this form the complex is called an amino-acyl tRNA (aa-tRNA).

The three main stages in each mechano-chemical cycle of a ribosome, shown in fig.2, are as follows: (i) selection of the cognate (i.e., correct) aa-tRNA, (ii) formation of the peptide bond between the amino acid brought in by the selected aa-tRNA and the elongating protein, (iii) translocation of the ribosome by one codon on its track. However, some of these steps consist of important sub-steps. Moreover, the aa-tRNA selected (erroneously) by the ribosome may not be the cognate tRNA; this leads to a branching of pathways. Such branching, in turn, gives rise to the possibility of more than one cyclic pathway for a ribosome in a given cycle.

Let us begin with the state labelled by "1"; both the E and A sites are empty while the site P is occupied as shown in fig.3. An incoming aa-tRNA molecule, bound to an elongation factor EF-Tu, occupies the site A; the resulting state is labelled by "2". The transition $1 \rightarrow 2$ takes place at the rate ω_a. However, not all incoming aa-tRNA molecules are automatically selected by the ribosome. In order to ensure translational *fidelity* [42–45] the ribosome deploys a quality control mechanism to ensure that the aa-tRNA selected is, indeed, cognate (i.e., carries the correct amino acid as dictated by the mRNA template). A non-cognate tRNA is rejected on the basis of codon-anticodon mismatch; the

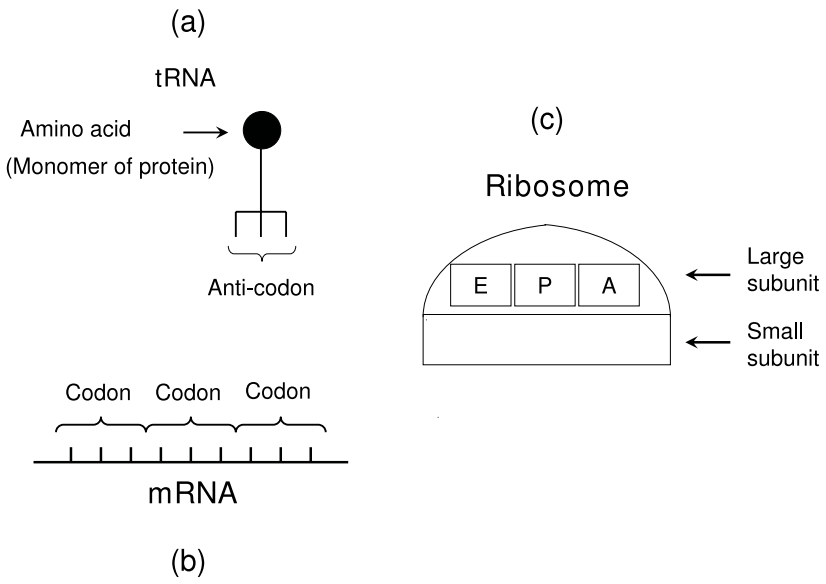

FIG. 1: Cartoons representing the main molecules and machinery involved in the process of *translation*.

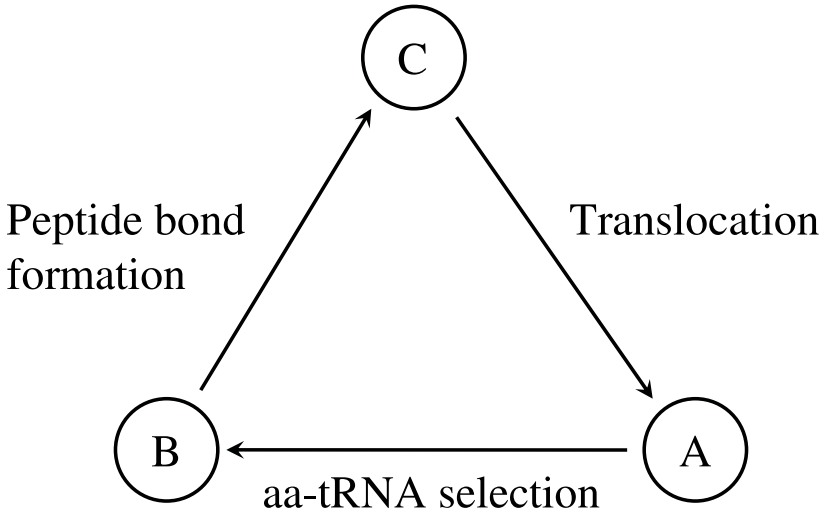

FIG. 2: Pictoral depiction of the three main stages in the chemo-mechanical cycle of a single ribosome (see the text for details).

corresponding transition $2 \to 1$ takes place at the rate ω_{r1}. However, if the aa-tRNA is not a non-cognate one, the GTP molecule bound to it is then hydrolyzed to GDP causing the irreversible transition $2 \to 3$ at the rate ω_{h1}. At this stage, kinetic proofreading can reject the tRNA if it is a near-cognate one; the transition $3 \to 1$ captures this phenomenon and takes place at the rate ω_{r2}. In our model we do not explicitly treat those sub-steps in which EF-TU and the products of the hydrolysis of GTP leave the ribosome. We'll later utilize the fact that ω_a is proportional to the concentration of the aa-tRNA molecules in the surrounding medium.

If the selected aa-tRNA is not rejected, it does not necessarily imply that it is cognate because, occasionally, even non-cognate or near-cognate aa-tRNA escapes the ribosomes quality control mechanism. The amino acid supplied by the selected aa-tRNA is then linked to the growing polypeptide by a peptide bond; this peptidyl transferase activity of the ribosome elongates the polypeptide by one monomer. The correct amino acid is incorporated at a rate ω_p whereas a wrong amino acid is incorporated at a rate Ω_p thereby giving rise to the two different branches of the mechano-chemical cycle of the ribosome; the third branch $3 \to 1$, however, ends a "futile" cycle. The only difference between the states 4 and 4^* is that the last amino acid in the polypeptide is correct in 4 but incorrect in 4^*. While the polypeptide gets elongated by one amino acid, a fresh molecule of GTP enters bound with an elongation factor EF-G. The arrival of GTP-bound EF-G is not treated explicitly in our model. Alternatively, ω_p (and Ω_p) is an effective rate

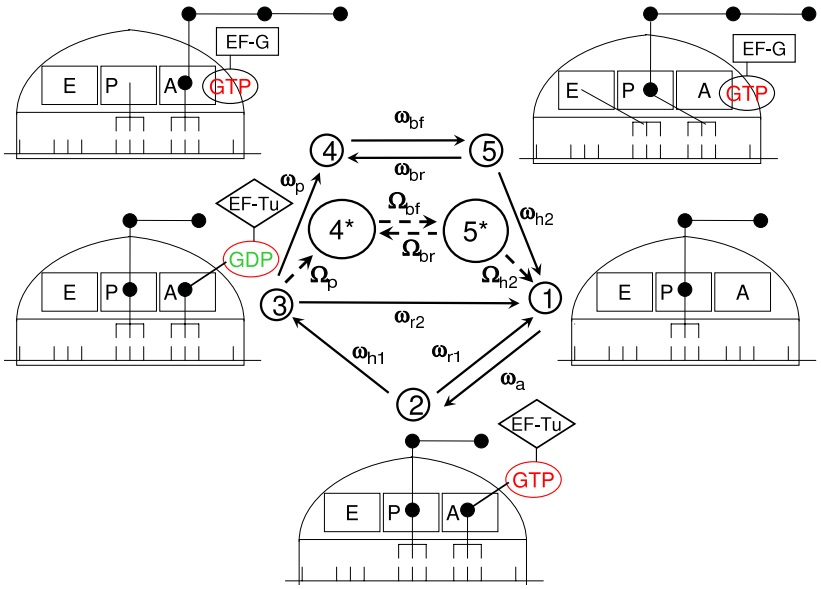

FIG. 3: Pictoral depiction of the main steps in the chemo-mechanical cycle of a single ribosome (see the text for details).

constant that accounts for both the polypeptide elongation and the arrival of the GTP-bound EF-G.

Next, spontaneous Brownian (relative) rotation of the two subunits of the ribosome coincides with the back-and-forth transition between the so-called "classical" and "hybrid" configurations of the two tRNA molecules. [46–56] In the classical configuration, both ends of the two tRNA molecules correspond to the locations of P and A sites. In contrast, in the hybrid configuration the ends of tRNA molecules interacting with the large subunit are found at the locations of E and P sites, respectively. The forward transition $4 \to 5$ takes place at the rate ω_{bf} along the correct branch (and at the rate Ω_{bf} along the wrong branch) whereas the reverse transition $5 \to 4$ takes place at the rate ω_{br} along the correct branch (and Ω_{br} along the wrong branch). The reversible transition $4 \rightleftharpoons 5$, which is caused by spontaneous Brownian fluctuations, does not need any free energy input from GTP hydrolysis.

Finally the hydrolysis of GTP drives the irreversible transition $5 \to 1$ which involves the translocation of the ribosome on its track by one codon and, simultaneously, that of the tRNAs inside the ribosome by one binding site following which the deacetylated (i.e., denuded of amino acid) tRNA exits from the E site. The rate of this transition is ω_{h2} or Ω_{h2} depending on whether the system is following the correct branch or the wrong branch. In our model, the transition $5 \to 1$ captures the hydrolysis of GTP, departure of the products of hydrolysis alongwith EF-G as well as the final exist of the deacetylated tRNA molecule from the E site.

The rate constant ω_a can be made identical for both species of amino acid monomers by maintaining their concentrations in the medium appropriately. The rate constant ω_{r1} refers only to the wrong amino acids (i.e., non-cognate tRNA) because, we assume, cognate tRNA is not rejected at all. Since the transition $2 \to 3$ accounts for the hydrolysis of a GTP molecule by the GTPase EF-Tu, the corresponding rate constant is ω_{h1}, irrespective of the identity of the attached aa-tRNA. In kinetic proofreading, the rate of rejection of the non-cognate tRNA is much higher than that of a cognate tRNA. For the sake of simplicity, we assume that the cognate tRNA is not rejected at all. Therefore, the rate constant ω_{r2} referers to the rejection of only non-cognate tRNA. For the remaining steps of the mechano-chemical cycle, the rate constants are ω_p, ω_{bf}, ω_{br} and ω_{h2} provided a cognate tRNA has been selected finally. On the other hand, the corresponding rate constants are Ω_p, Ω_{bf}, Ω_{br} and Ω_{h2}, respectively, if a non-cognate tRNA escapes rejection by the quality control system of the ribosome. Since the last step involves not only hydrolysis of GTP by the GTPase EF-G, but also translocation of the ribosome and the tRNA molecules, the rate constants ω_{h2} and Ω_{h2} need not be equal, in general.

Thus our model is an extension of the generic models for molecular motors based on stochastic chemical kinetic approach which was pioneered by Fisher and Kolomeisky [57, 58]. Following Hill [59] the mechano-chemical kinetics of a ribosome in our model can be regarded as a composite of the four cycles shown in Fig.4.

All the numerical data generated from the analytical expressions for the graphical plots have the following set of values of the rate constants (except in the figures where $f(t)$ has been plotted for several different values of the parameters ω_p and ω_{r2}) : $\omega_a = 25\text{s}^{-1}$, $\omega_{r1} = 10\text{s}^{-1}$, $\omega_{h1} = 25\text{s}^{-1}$, $\Omega_p = 40\text{s}^{-1}$, $\omega_{bf} = \omega_{br} = 25\text{s}^{-1}$, $\Omega_{bf} = \Omega_{br} = 10\text{s}^{-1}$, $\omega_{h2} = 25\text{s}^{-1}$, $\Omega_{h2} = 10\text{s}^{-1}$. The value of $\omega_a = 25\text{s}^{-1}$ is identical to that used in our earlier papers (see [25, 26] and the references therein). For the purpose of plotting our results, the magnitude of the other parameters have been chosen

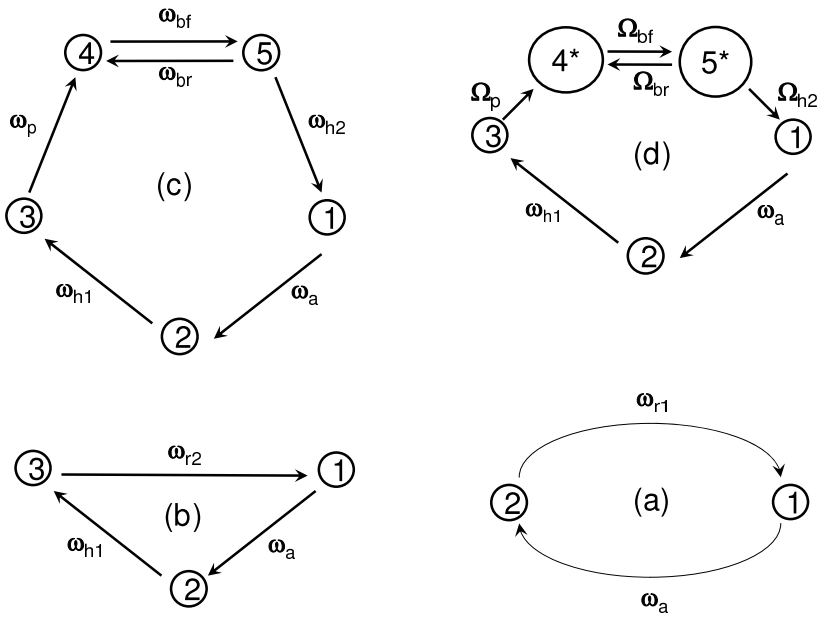

FIG. 4: The full mechano-chemical kinetic of a ribosome during the elongation state, as modelled in Fig.3, can be regarded as a composite of at least four different cycles shown in (a)-(d). Among these, both (a) and (b) are unproductive in the sense that these lead to neither elongation of the polypeptide nor forward stepping of the ribosome. However, (b) is "futile" because it dissipates the free energy input from the hydrolysis of a GTP molecule whereas no fuel is wasted in (a) . In contrast, both (c) and (d) lead to elongation of the polypeptide and forward stepping of the ribosome by hydrolysing two molecules of GTP; however, (c) incorporates the correct amino acid whereas (d) incorporated a wrong amino acid into the growing polypeptide.

to be comparable to that of ω_a. The values of some of the parameters, and the ranges over which some of these have been varied, may be unrealistically high or low. But, this deliberate choice has been motivated by our intention to demonstrate graphically the interplay of various kinetic processes in translation.

III. DWELL TIME DISTRIBUTION

For the convenience of mathematical calculations, we assume that, after reaching the state 5 (or 5^*) at location j the system makes a transition to a hypothetical state $\widetilde{1}$ at location $j+1$ which, then, relaxes to the state 1, at the same location, at the rate δ. At the end of the calculation our model is recovered by setting $\delta \to \infty$.

Suppose $P_\mu(j,t)$ denote the probability at time t that the ribosome is in the "chemical" state μ and is decoding the j-th codon. Let us use the symbol $\widetilde{P}_1(j+1,t)$ to denote the probability of finding the ribosome in the hypothetical state $\widetilde{1}$ at time t while decoding the $j+1$-th codon. The time taken by the ribosome to reach the state $\widetilde{1}$ at $j+1$, starting from the initial state 1 at j, defines its time of dwell at the j-th codon. Since, in this context, all the "chemical" states, except $\widetilde{1}$ refer to the j-th codon while $\widetilde{1}$ corresponds to the $j+1$-th codon, from now onwards we drop the site index j (and $j+1$) to keep the notations simple.

The master equations governing the time evolution of the probabilities $P_\mu(t)$ can be written as

$$\frac{dP_1(t)}{dt} = -\omega_a P_1(t) + \omega_{r1} P_2(t) + \omega_{r2} P_3(t) \tag{1}$$

$$\frac{dP_2(t)}{dt} = \omega_a P_1(t) - (\omega_{r1} + \omega_{h1}) P_2(t) \tag{2}$$

$$\frac{dP_3(t)}{dt} = \omega_{h1} P_2(t) - (\omega_p + \Omega_p + \omega_{r2}) P_3(t) \tag{3}$$

$$\frac{dP_4(t)}{dt} = \omega_p P_3(t) - \omega_{bf} P_4(t) + \omega_{br} P_5(t) \tag{4}$$

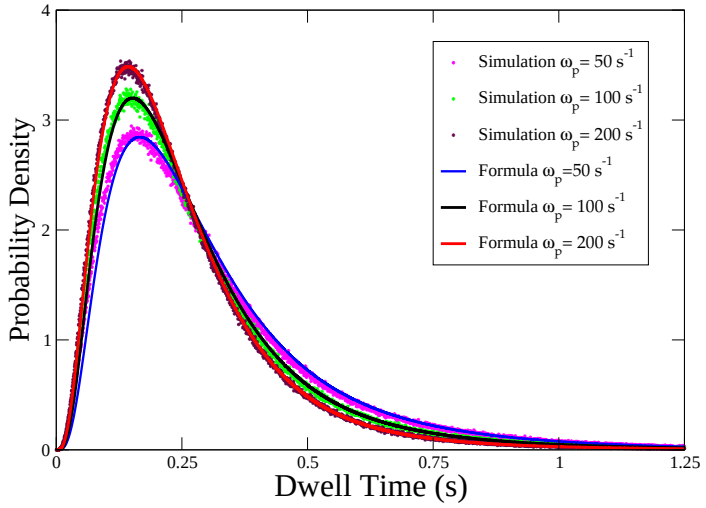

FIG. 5: The probability density of the dwell times are plotted for a few different values of the parameter ω_p.

$$\frac{dP_5(t)}{dt} = \omega_{bf} P_4(t) - (\omega_{h2} + \omega_{br}) P_5(t) \tag{5}$$

$$\frac{dP_4^*(t)}{dt} = \Omega_p P_3(t) - \Omega_{bf} P_4^*(t) + \Omega_{br} P_5^*(t) \tag{6}$$

$$\frac{dP_5^*(t)}{dt} = \Omega_{bf} P_4^*(t) - (\Omega_{h2} + \Omega_{br}) P_5^*(t) \tag{7}$$

$$\frac{d\widetilde{P_1}(t)}{dt} = \omega_{h2} P_5(t) + \Omega_{h2} P_5^*(t) \tag{8}$$

Because of the normalization condition

$$\sum_{\mu=1}^{5} P_\mu(t) + P_4^*(t) + P_5^*(t) + \widetilde{P_1}(t) = 1 \tag{9}$$

not all the equations (1)-(8) above are independent of each other.

For the calculation of the dwell time, we impose the initial conditions

$$P_1(0) = 1, \text{ and } P_2(0) = P_3(0) = P_4(0) = P_5(0) = P_4^*(0) = P_5^*(0) = \widetilde{P_1}(0) = 0 \tag{10}$$

Suppose, $f(t)$ is the probability density of the dwell times. Then, the probability of adding one amino acid to the growing polypeptide in the time interval between t and $t + \Delta t$ is $f(t)\Delta t$ where

$$f(t) = \frac{\Delta \widetilde{P_1}(t)}{\Delta t} = \omega_{h2} P_5(t) + \Omega_{h2} P_5^*(t) \tag{11}$$

The calculation of the DTD [60–65] is essentially that of a distribution of first-passage times [66].

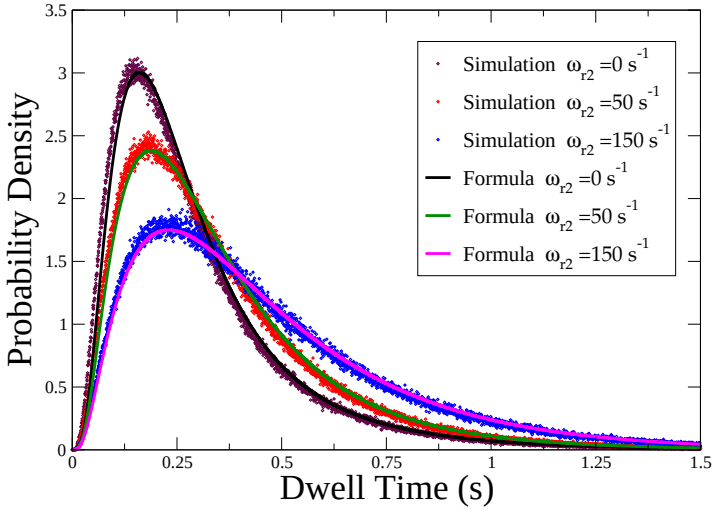

FIG. 6: The probability density of the dwell times are plotted for a few different values of the parameter ω_{r2}.

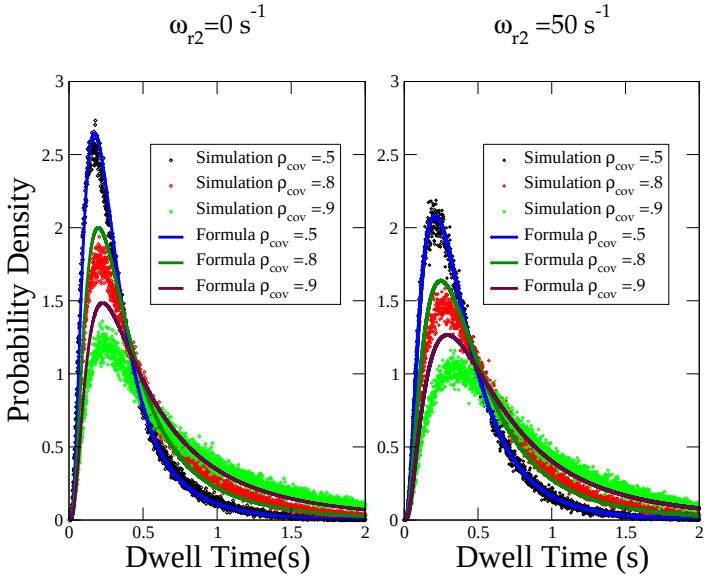

FIG. 7: The probability density of the dwell times are plotted for a few different values of the coverage density ρ_{cov} of the ribosomes.

The *exact* probability density of the dwell times is given by

$$\begin{aligned} f(t) &= \left[\frac{\omega_{h2}\omega_{bf}\omega_p\omega_{h1}\omega_a}{(\omega_1-\omega_2)(\omega_1-\omega_3)(\omega_1-\omega_4)(\omega_1-\omega_5)}\right]e^{-\omega_1 t} + \left[\frac{\Omega_{h2}\Omega_{bf}\Omega_p\omega_{h1}\omega_a}{(\omega_1-\omega_2)(\omega_1-\omega_3)(\omega_1-\Omega_4)(\omega_1-\Omega_5)}\right]e^{-\omega_1 t} \\ &+ \left[\frac{\omega_{h2}\omega_{bf}\omega_p\omega_{h1}\omega_a}{(\omega_2-\omega_3)(\omega_2-\omega_4)(\omega_2-\omega_5)(\omega_2-\omega_1)}\right]e^{-\omega_2 t} + \left[\frac{\Omega_{h2}\Omega_{bf}\Omega_p\omega_{h1}\omega_a}{(\omega_2-\omega_3)(\omega_2-\Omega_4)(\omega_2-\Omega_5)(\omega_2-\omega_1)}\right]e^{-\omega_2 t} \\ &+ \left[\frac{\omega_{h2}\omega_{bf}\omega_p\omega_{h1}\omega_a}{(\omega_3-\omega_4)(\omega_3-\omega_5)(\omega_3-\omega_1)(\omega_3-\omega_2)}\right]e^{-\omega_3 t} + \left[\frac{\Omega_{h2}\Omega_{bf}\Omega_p\omega_{h1}\omega_a}{(\omega_3-\Omega_4)(\omega_3-\Omega_5)(\omega_3-\omega_1)(\omega_3-\omega_2)}\right]e^{-\omega_3 t} \\ &+ \left[\frac{\omega_{h2}\omega_{bf}\omega_p\omega_{h1}\omega_a}{(\omega_4-\omega_5)(\omega_4-\omega_1)(\omega_4-\omega_2)(\omega_4-\omega_3)}\right]e^{-\omega_4 t} + \left[\frac{\Omega_{h2}\Omega_{bf}\Omega_p\omega_{h1}\omega_a}{(\Omega_4-\Omega_5)(\Omega_4-\omega_1)(\Omega_4-\omega_2)(\Omega_4-\omega_3)}\right]e^{-\Omega_4 t} \\ &+ \left[\frac{\omega_{h2}\omega_{bf}\omega_p\omega_{h1}\omega_a}{(\omega_5-\omega_1)(\omega_5-\omega_2)(\omega_5-\omega_3)(\omega_5-\omega_4)}\right]e^{-\omega_5 t} + \left[\frac{\Omega_{h2}\Omega_{bf}\Omega_p\omega_{h1}\omega_a}{(\Omega_5-\omega_1)(\Omega_5-\omega_2)(\Omega_5-\omega_3)(\Omega_5-\Omega_4)}\right]e^{-\Omega_5 t} \end{aligned} \tag{12}$$

where ω_1,ω_2 and ω_3 are solution of the cubic equation

$$\begin{aligned} &\omega^3 - \omega^2(\omega_{r1}+\omega_{h1}+\omega_a+\omega_{r2}+\omega_p+\Omega_p) + \omega(\omega_{h1}\omega_a+\omega_{r2}\omega_{r1}+\omega_{r2}\omega_{h1}+\omega_{r2}\omega_a \\ &+ \omega_p\omega_{r1}+\omega_p\omega_{h1}+\omega_p\omega_a+\Omega_p\omega_{r1}+\Omega_p\omega_{h1}+\Omega_p\omega_a) - \Omega_p\omega_{h1}\omega_a+\omega_p\omega_{h1}\omega_a = 0, \end{aligned} \tag{13}$$

ω_4 and ω_5 are the solution of the quadratic equation

$$\omega^2 - \omega(\omega_{h2}+\omega_{br}+\omega_{bf}) + \omega_{h2}\omega_{bf} = 0 \tag{14}$$

and Ω_4 and Ω_5 are the solution of the quadratic equation

$$\Omega^2 - \Omega(\Omega_{h2}+\Omega_{br}+\Omega_{bf}) + \Omega_{h2}\Omega_{bf} = 0 \tag{15}$$

Some of the details of this derivation are given in the appendix. Note that the problem of determining the rates ω_i $(i = 1, 2, 3, 4, 5)$ in terms of the rate constants of the model is similar to that of expressing the normal modes of vibration of a set of coupled harmonic oscillators. It is the "backward" reactions in the mechano-chemical cycle of our model which play the role of coupling of the harmonic oscillators. For example, if $\Omega_p = 0$ and simultaneously, $\omega_{r1} = \omega_{r2} = \omega_{br} = 0$, the expressions for ω_i $(i = 1, 2, 3, 4, 5)$ reduce to the simple form $\omega_1 = \omega_a$, $\omega_2 = \omega_{h1}$, $\omega_3 = \omega_p$, $\omega_4 = \omega_{bf}$, and $\omega_5 = \omega_{h2}$.

The distribution (12) is plotted in Fig.5 for a few different values of the parameter ω_p. Note that

$$\phi = \omega_p/(\omega_p+\Omega_p) \tag{16}$$

is a measure of the fidelity of translation. Therefore, increasing ω_p, keeping Ω_p fixed, enhances translational fidelity. Moreover, a higher ω_p also corresponds to faster peptidyl transferase reaction. Therefore, the trend of variation of the most probable dwell time with ω_p is consistent with the intuitive expectation that the slower is the peptidyl transferase reaction, the longer is the dwell time.

The kinetic parameter ω_{r2} is a measure of the rate of rejection of the aa-tRNA by kinetic proofreading. Consequently, the effect of the variation of the ω_{r2} on the most probable dwell time is opposite to that of ω_p (see Fig.6); the higher is the frequency of tRNA rejection by kinetic proofreading, the longer is the dwell time.

IV. MEAN RATE OF POLYMERIZATION: A MICHAELIS-MENTEN-LIKE EQUATION

The average Dwell time can be calculated by substituting (12) into the definition

$$\langle t\rangle = \int_0^{+\infty} t f(t)\, dt. \tag{17}$$

Hence, the expression for $\langle t\rangle$

$$\langle t\rangle = \frac{1}{\omega_1}+\frac{1}{\omega_2}+\frac{1}{\omega_3}+\frac{\omega_p}{\omega_p+\Omega_p}\left(\frac{1}{\omega_4}+\frac{1}{\omega_5}\right)+\frac{\Omega_p}{\omega_p+\Omega_p}\left(\frac{1}{\Omega_4}+\frac{1}{\Omega_5}\right) \tag{18}$$

written in terms of $\omega_1, \omega_2, \omega_3, \omega_4, \omega_5, \Omega_4$ and Ω_5 has a clear physical meaning. In the special case $\Omega_p = 0$, $\langle t \rangle = \sum_{i=1}^{5} \omega_i^{-1}$. However, if $\Omega_p \neq 0$, then the sum $\omega_4^{-1} + \omega_5^{-1}$ is replaced by the last two terms of (18) where $\omega_p/(\omega_p + \Omega_p)$ and $\Omega_p/(\omega_p + \Omega_p)$ are the weight factors associated with the two paths emanating from the state labelled by 3.

Finally, in terms of the rate constants for the mechano-chemical transitions in the model depicted in fig.3

$$\begin{aligned} \langle t \rangle &= \frac{1}{V} = \frac{1}{\omega_a}\left(1 + \frac{\omega_{r1}}{\omega_{h1}}\right)\left(1 + \frac{\omega_{r2}}{\omega_p + \Omega_p}\right) + \frac{1}{\omega_{h1}}\left(1 + \frac{\omega_{r2}}{\omega_p + \Omega_p}\right) + \frac{1}{\omega_p + \Omega_p} \\ &+ \frac{\omega_p}{\omega_p + \Omega_p}\left[\frac{1}{\omega_{bf}}\left(1 + \frac{\omega_{br}}{\omega_{h2}}\right) + \frac{1}{\omega_{h2}}\right] + \frac{\Omega_p}{\omega_p + \Omega_p}\left[\frac{1}{\Omega_{bf}}\left(1 + \frac{\Omega_{br}}{\Omega_{h2}}\right) + \frac{1}{\Omega_{h2}}\right] \end{aligned} \tag{19}$$

Next we'll show that the equation (19) can be re-expressed in a form that resembles the Michaelis-Menten equation for simple enzymatic reactions [28]. Consider an enzymatic reaction of the type

$$E + S \underset{\omega_{-1}}{\overset{\omega_{+1}}{\rightleftharpoons}} ES \overset{\omega_{+2}}{\rightarrow} E + P \tag{20}$$

where E is the enzyme, S is the substrate and P is the product of the reaction catalyzed by E. Given that the total initial concentration of the enzyme is $[E]_0$, the rate V of this reaction is given by

$$\frac{1}{V} = \frac{1}{V_{max}} + \frac{K_M}{V_{max}} \frac{1}{[S]} \tag{21}$$

where the maximum possible rate of the reaction is

$$V_{max} = \omega_{+2}[E]_0 \equiv \tilde{\omega}_2 \tag{22}$$

and the Michaelis constant K_M is given by

$$K_M = \frac{\omega_{-1} + \omega_{+2}}{\omega_{+1}} \tag{23}$$

In the case of our model, we assume that the "pseudo" first order rate constant ω_a can be written as $\omega_a = \omega_a^0 [tRNA]$ where $[tRNA]$ is the concentration of tRNA molecules in the solution. Treating tRNA molecules as the analogues of the substrates in an enzymatic reaction, equation (19) can be re-expressed as a Michaelis-Menten-like Equation [28]

$$\langle t \rangle = \frac{1}{V_{max}} + \frac{K_M}{V_{max}} \frac{1}{[tRNA]} \tag{24}$$

where

$$\begin{aligned} \frac{1}{V_{max}} &= \frac{1}{\omega_2^{eff}} = \frac{1}{\omega_{h1}}\left(1 + \frac{\omega_{r2}}{\omega_p + \Omega_p}\right) + \frac{1}{\omega_p + \Omega_p} \\ &+ \frac{\omega_p}{\omega_p + \Omega_p}\left[\frac{1}{\omega_{bf}}\left(1 + \frac{\omega_{br}}{\omega_{h2}}\right) + \frac{1}{\omega_{h2}}\right] + \frac{\Omega_p}{\omega_p + \Omega_p}\left[\frac{1}{\Omega_{bf}}\left(1 + \frac{\Omega_{br}}{\Omega_{h2}}\right) + \frac{1}{\Omega_{h2}}\right] \end{aligned} \tag{25}$$

and the Michaelis constant

$$K_M = \frac{\omega_{-1}^{eff} + \omega_2^{eff}}{\omega_a^0} \tag{26}$$

with

$$\omega_{-1}^{eff} = \left(\frac{\omega_{r1}}{\omega_{h1}} + \frac{\omega_{r2}}{\omega_p + \Omega_p} + \frac{\omega_{r1}\omega_{r2}}{\omega_{h1}(\omega_p + \Omega_p)}\right)\omega_2^{eff} \tag{27}$$

Thus, the mean dwell time for the ribosomes follows a Michaelis-Mentan-like equation. This result is consistent with the experimental observations in recent years [67–72] that, in spite of the fluctuations of an enzymatic reaction catalyzed by a *single* enzyme molecule, the average rate of the reaction is, most often, given by the Michaelis-Menten equation. What makes the Michaelis-Menten-like equation for the ribosome even more interesting is the fact that a single ribosome is not a single enzyme molecule, but it provides a platform for the coordinated operation of several bio-catalysts.

V. EFFECTS OF CROWDING ON THE DWELL TIME DISTRIBUTION

It is well known that most often a large number of ribosomes simultaneously move on the same mRNA track each polymerizing one copy of the same protein. This phenomenon is usually referred to as ribosome traffic because of its superficial similarity with vehicular traffic on highways [26, 29–41] . Suppose, ℓ denotes the number of codons that a ribosome can cover simultaneously. Extending the prescription used in our earlier works on ribosome traffic [26] for capturing the steric interactions of the ribosomes, we replace the equations (5), (7 and (8) by

$$\frac{dP_5(i,t)}{dt} = \omega_{bf}P_4(i,t) - \omega_{br}P_5(i,t) - \omega_{h2}P_5(i,t)Q(\underline{\mathrm{i}}|i+\ell) \tag{28}$$

$$\frac{dP^*_5(i,t)}{dt} = \Omega_{bf}P^*_4(i,t) - \Omega_{br}P^*_5(i,t) - \Omega_{h2}P^*_5(i,t)Q(\underline{\mathrm{i}}|i+\ell) \tag{29}$$

$$\frac{d\widetilde{P_1}(i,t)}{dt} = \Big(\omega_{h2}P_5(i-1,t) + \Omega_{h2}P^*_5(i-1,t)\Big)Q(\underline{\mathrm{i\text{-}1}}|i-1+\ell) \tag{30}$$

where $Q(\underline{\mathrm{i}}|j) = 1 - P(\underline{\mathrm{i}}|j)$ is the conditional probability that, given a ribosome in site i, site j is empty. All the other equations for $P_\mu(i,t)$ remain unchanged. Note that these equations have been written under the *mean-field approximation*.

In the limit $L \to \infty$, all the sites are treated on the same footing so that the site-dependence of $P_\mu(i,t)$ drops out. In this limit, Q takes the simple form [26]

$$Q(\underline{\mathrm{i}}|i+\ell) = \frac{1-\rho\ell}{1+\rho-\rho\ell}. \tag{31}$$

where ρ is the number density of the ribosomes (i.e., number of ribosomes per unit length of the mRNA track).

Therefore, in ribosome traffic the distribution of the dwell times of the ribosomes is given by the expression (12) where ω_{h2} and Ω_{h2} are replaced by $\omega_{h2}Q$ and $\Omega_{h2}Q$, respectively. Using the expression (31), we get the DTD for the given number density ρ of the ribosomes. For the purpose of graphical demostration of the effects of ribosome crowding on the DTD, we use the *coverage* density $\rho_{cov} = \rho\,\ell$. In Fig.7 we plot the DTD for a few different values of ρ_{cov}. The higher is the density, the stronger is the hindrance and longer is the dwell time. Moreover, higher coverage density introduces stronger correlations which our mean-field equations ignore. Consequently, our analytical predictions, based on equations written under the mean-field approximation, deviate more and more from the corresponding simulation data as the coverage density increases.

VI. COMPARISON WITH EXPERIMENTAL DATA

The distribution of dwell times involves essentially five different rate-determining parameters ω_i $(i = 1, 2, 3, 4, 5)$ if the translational fidelity is perfect. This is consistent with the earlier observation [24] that the best fit to the simulation data was obtained with five rate-determining parameters. However, the dwell time distribution obtained from the single-molecule experiments (more precisely, single-ribosome manipulation) fit reasonably well with a difference of just two exponentials [23]. This strongly indicates the possibility that only two of the five rate-determining parameters were rate-limiting under the conditions maintained in those experiments. However, for a quantitative testing of the predictions of our theoretical model, one should use a mRNA template with a homogeneous codon sequence and only two species of aa-tRNA one of which is cognate (corresponding to the codons in the coding sequence of the mRNA) and the other is either near-cognate or non-cognate.

In order to clarify the proposed experimental set up, let us consider the concrete example shown schematically in fig. 8. This example is essentially the protocols used by Uemura et al. [20] in their single-molecule studies of translation in real time. The actual coding sequence to be translated consists of n_c number of identical codons; in fig.8 $n_c = 6$ and each codon is UUU which codes for the amino acid Phenylalanine (abbreviated *Phe* or **F**). The coding sequence is preceeded by a start codon AUG and is followed by a stop codon UAA. The start codon itself is preceeded by an untranslated region (UTR) at the 5'-end of the mRNA; this is required for assembling the ribosome and for stabilizing the pre-initiation complex. At the 3'-end, the stop codon is followed by a sequence of n_{nc} non-coding codons UUU ($n_{nc} = 4$ in fig.8); this region merely ensures the absence of any "edge effect", i.e., the translation is not affected when the ribosome approaches the 3'-end of the codong sequence. A good choice for the corresponding near-cognate

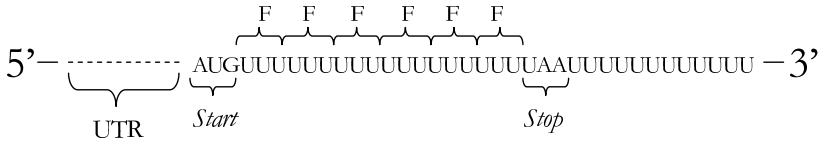

FIG. 8: A schematic description of a mRNA with homogeneous (poly-U) coding sequence (adapted from refs.[20, 21]).

tRNA would be tRNA^{Leu} because it is cognate for the codon CUU which codes for *Leucine* (abbreviated **L**). The two distinct species of aa-tRNA should be labelled by fluorescent dye molecules of two different colors which could be, for example, Cy5 (red) and Cy3 (green). Equal concentrations of Cy5-labelled ternary complexe aa-tRNA^{Phe}-EF-Tu-GTP and Cy3-labelled ternary complex aa-tRNA^{Leu}-EF-Tu-GTP should be made available in the medium surrounding the ribosome to avoid any bias arising from difference in their concentrations. The color of the fluorescence pulse identifies the amino acid monomer species that elongates the polypeptide by one unit; monitoring the colors of the fluorescence pulses one would get an estimate of the translational fidelity ϕ. Moreover, the time interval between the arrival of the successive aa-tRNA molecules provides an estimate of the dwell times of the ribosome. Thus, using this optical technique one would get not only the DTD, but also the fidelity of translation. Usually the coding sequence of such poly-U mRNA strands is quite short. Therefore, for collecting enough data to extract the DTD, the experiment has to be repeated sufficiently large number of times.

The effects of kinetic proofreading on the rate of translational error has been investigated experimentally by several different methods in the last three decades. However, most of those methods (see, for example, ref.[73, 74]) require bulk samples. But, the more recent single-molecule FRET technique used in the study of tRNA selection [19] seems to be more suitable for testing our predictions on the effects of kinetic proofreading on the DTD.

The cluster of ribosomes translating the same mRNA simultaneously is usually referred to as a *polysome*. For studying the effects of ribosome crowding on the DTD, one has to measure simultaneously the DTD and the polysome size [75].

VII. SUMMARY AND CONCLUSION

In this paper we have presented a theoretical model of translation that captures all the main steps in the mechano-chemical cycle of a ribosome during the elongation stage. This model also accounts for translational fidelity, kinetic proofreading and the crowding of the ribosomes on the same mRNA track. In principle, this model can be extended, by increasing the number of "chemical" states, to account for some of the sub-steps which have not been treated explicitly in the version of the model presented here.

In spite of the details already incorporated in this model, we have suceeded in carrying out an *analytical* calculation of the distribution of the dwell times of the ribosomes at the successive codons. We have compared this theoretical estimate of the DTD with the corresponding numerical data which we have obtained from direct computer simulation of the model. If the motion of the ribosome is not hindered by the presence of any other ribosome on the same mRNA track, our analytical treatment yields the *exact* expression for the distribution for the times of its dwell at the successive codons. In this case, excellent agreement between theoretical prediction and simulation data is observed provided the data are averaged over sufficiently large number of samples.

However, because of the mean-field approximation made in capturing the effects of crowding of the ribosomes the corresponding analytical expression is approximate. Therefore, the higher is the coverage density, the larger is the deviation of the analytical estimate from the simulation data which are averaged over many samples.

We have analyzed the dependence of the DTD on some of the crucially important kinetic parameters of the model to elucidate the physical implications of the result. Our results are in good qualitative agreement with the experimental data reported in the literature [23, 24]. However, for the reasons explained in the sections I and II, it is not possible to compare these experimental data quantitatively with the analytical expressions of DTD which we have reported in this paper. We hope our theoretical predictions will stimulate further experimental studies along the lines suggested briefly in section VI although some technical hurdles may hinder quick progress. A combination of the single-ribosome experiments and bulk measurements may be required for comparing the theoretically predicted variation of the DTD with the concentrations of tRNA, GTP and other key molecules involved in translation as well as with the increase of futile cycles and crowding.

It would also be desirable to extend our model in future to account for some important features of translation; some of these possible extentions are listed below. (i) Capturing the sequence heterogeneity of real mRNA templates will

open up larger number of branched pathways in Fig.3, each corresponding to a distinct species (cognate, non-cognate or near-cognate) of amino acid. Moreover, at each step of the ribosome, the rate constants for the correct and incorrect pathways will also depend on the codon under consideration. (ii) The interaction of the growing polypeptide with the exit tunnel in the ribosome and the spontaneous folding of the nascent protein as it comes out of the tunnel may affect the rate of translation. It may be possible to capture these effects by making some of the relevant rate constants, e.g., ω_{h2}, Ω_{h2}, etc. on the instantaneous length of the growing polypeptide which, in turn, is identical to the length of the codon sequence already translated by the ribosome. (iii) Maintaining correct reading frame on a sequence-homogeneous mRNA (e.g., poly-U) may be more difficult than on an inhomogeneous sequence. It may be desirable to extend our model allowing the possibility of frameshift errors [76] although, at present, the prescription for this extension is not obvious. The DTD for such a "realistic model" may be obtained numerically because an *analytical* derivation of the general expression may not be possible in the forseeable future.

Acknowledgements: One of the authors (DC) thanks Joachim Frank and Joseph D. Puglisi for useful correspondences.

Appendix

Solving the equations (1)-(7) under the initial condition (10) we get

$$P_1(t) = C_1 e^{-\omega_1 t} + C_2 e^{-\omega_2 t} + C_3 e^{-\omega_3 t} \tag{32}$$

$$P_2(t) = \frac{C_1\omega_a e^{-\omega_1 t}}{\omega_{r1}+\omega_{h1}-\omega_1} + \frac{C_2\omega_a e^{-\omega_2 t}}{\omega_{r1}+\omega_{h1}-\omega_2} + \frac{C_3\omega_a e^{-\omega_3 t}}{\omega_{r1}+\omega_{h1}-\omega_3} \tag{33}$$

$$\begin{aligned} P_3(t) &= \frac{C_1\omega_{h1}\omega_a e^{-\omega_1 t}}{(\omega_{r1}+\omega_{h1}-\omega_1)(\omega_{r2}+\omega_p+\Omega_p-\omega_1)} + \frac{C_2\omega_{h1}\omega_a e^{-\omega_2 t}}{(\omega_{r1}+\omega_{h1}-\omega_2)(\omega_{r2}+\omega_p+\Omega_p-\omega_2)} \\ &+ \frac{C_3\omega_{h1}\omega_a e^{-\omega_3 t}}{(\omega_{r1}+\omega_{h1}-\omega_3)(\omega_{r2}+\omega_p+\Omega_p-\omega_3)} \end{aligned} \tag{34}$$

$$\begin{aligned} P_4(t) &= \frac{C_1\omega_p\omega_{h1}\omega_a(\omega_{h2}+\omega_{br}-\omega_1)e^{-\omega_1 t}}{(\omega_{r1}+\omega_{h1}-\omega_1)(\omega_{r2}+\omega_p+\Omega_p-\omega_1)(\omega_4-\omega_1)(\omega_5-\omega_1)} \\ &+ \frac{C_2\omega_p\omega_{h1}\omega_a(\omega_{h2}+\omega_{br}-\omega_2)e^{-\omega_2 t}}{(\omega_{r1}+\omega_{h1}-\omega_2)(\omega_{r2}+\omega_p+\Omega_p-\omega_2)(\omega_4-\omega_2)(\omega_5-\omega_2)} \\ &+ \frac{C_3\omega_p\omega_{h1}\omega_a(\omega_{h2}+\omega_{br}-\omega_3)e^{-\omega_3 t}}{(\omega_{r1}+\omega_{h1}-\omega_3)(\omega_{r2}+\omega_p+\Omega_p-\omega_3)(\omega_4-\omega_3)(\omega_5-\omega_3)} \\ &+ C_4 e^{-\omega_4 t} + C_5 e^{-\omega_5 t} \end{aligned} \tag{35}$$

$$\begin{aligned} P_5(t) &= \frac{C_1\omega_{bf}\omega_p\omega_{h1}\omega_a e^{-\omega_1 t}}{(\omega_{r1}+\omega_{h1}-\omega_1)(\omega_{r2}+\omega_p+\Omega_p-\omega_1)(\omega_4-\omega_1)(\omega_5-\omega_1)} \\ &+ \frac{C_2\omega_{bf}\omega_p\omega_{h1}\omega_a e^{-\omega_2 t}}{(\omega_{r1}+\omega_{h1}-\omega_2)(\omega_{r2}+\omega_p+\Omega_p-\omega_2)(\omega_4-\omega_2)(\omega_5-\omega_2)} \\ &+ \frac{C_3\omega_{bf}\omega_p\omega_{h1}\omega_a e^{-\omega_3 t}}{(\omega_{r1}+\omega_{h1}-\omega_3)(\omega_{r2}+\omega_p+\Omega_p-\omega_3)(\omega_4-\omega_3)(\omega_5-\omega_3)} \\ &+ \frac{C_4\omega_{bf}e^{-\omega_4 t}}{\omega_{h2}+\omega_{br}-\omega_4} + \frac{C_5\omega_{bf}e^{-\omega_5 t}}{\omega_{h2}+\omega_{br}-\omega_5} \end{aligned} \tag{36}$$

$$\begin{aligned} P_4^*(t) &= \frac{C_1\Omega_p\omega_{h1}\omega_a(\Omega_{h2}+\Omega_{br}-\omega_1)e^{-\omega_1 t}}{(\omega_{r1}+\omega_{h1}-\omega_1)(\omega_{r2}+\omega_p+\Omega_p-\omega_1)(\Omega_4-\omega_1)(\Omega_5-\omega_1)} \\ &+ \frac{C_2\Omega_p\omega_{h1}\omega_a(\Omega_{h2}+\Omega_{br}-\omega_2)e^{-\omega_2 t}}{(\omega_{r1}+\omega_{h1}-\omega_2)(\omega_{r2}+\omega_p+\Omega_p-\omega_2)(\Omega_4-\omega_2)(\Omega_5-\omega_2)} \\ &+ \frac{C_3\Omega_p\omega_{h1}\omega_a(\Omega_{h2}+\Omega_{br}-\omega_3)e^{-\omega_3 t}}{(\omega_{r1}+\omega_{h1}-\omega_3)(\omega_{r2}+\omega_p+\Omega_p-\omega_3)(\Omega_4-\omega_3)(\Omega_5-\omega_3)} \\ &+ D_4 e^{-\Omega_4 t} + D_5 e^{-\Omega_5 t} \end{aligned} \tag{37}$$

$$
\begin{aligned}
P_5^*(t) &= \frac{C_1\Omega_{bf}\Omega_p\omega_{h1}\omega_a e^{-\omega_1 t}}{(\omega_{r1}+\omega_{h1}-\omega_1)(\omega_{r2}+\omega_p+\Omega_p-\omega_1)(\Omega_4-\omega_1)(\Omega_5-\omega_1)} \\
&+ \frac{C_2\Omega_{bf}\Omega_p\omega_{h1}\omega_a e^{-\omega_2 t}}{(\omega_{r1}+\omega_{h1}-\omega_2)(\omega_{r2}+\omega_p+\Omega_p-\omega_2)(\Omega_4-\omega_2)(\Omega_5-\omega_2)} \\
&+ \frac{C_3\Omega_{bf}\Omega_p\omega_{h1}\omega_a e^{-\omega_3 t}}{(\omega_{r1}+\omega_{h1}-\omega_3)(\omega_{r2}+\omega_p+\Omega_p-\omega_3)(\Omega_4-\omega_3)(\Omega_5-\omega_3)} \\
&+ \frac{D_4\Omega_{bf}e^{-\Omega_4 t}}{\Omega_{h2}+\Omega_{br}-\Omega_4} + \frac{D_5\Omega_{bf}e^{-\Omega_5 t}}{\Omega_{h2}+\Omega_{br}-\Omega_5}
\end{aligned} \tag{38}
$$

where ω_1, ω_2 and ω_3 are the solutions of the cubic equation (13) while ω_4, ω_5 are the solutions of the quadratic equation (14) and Ω_4, Ω_5 are the solutions of the quadratic equation (15). The coefficients C_ν ($\nu = 1, 2, ..., 5$) and D_4, D_5, which are determined by the initial condition (10), are as follows:

$$C_1 = \frac{(\omega_{r1}+\omega_{h1}-\omega_1)(\omega_{r2}+\omega_p+\Omega_p-\omega_1)}{(\omega_2-\omega_1)(\omega_3-\omega_1)} \tag{39}$$

$$C_2 = \frac{(\omega_{r1}+\omega_{h1}-\omega_2)(\omega_{r2}+\omega_p+\Omega_p-\omega_2)}{(\omega_3-\omega_2)(\omega_1-\omega_2)} \tag{40}$$

$$C_3 = \frac{(\omega_{r1}+\omega_{h1}-\omega_3)(\omega_{r2}+\omega_p+\Omega_p-\omega_3)}{(\omega_1-\omega_3)(\omega_2-\omega_3)} \tag{41}$$

$$C_4 = \frac{(\omega_{h2}+\omega_{br}-\omega_4)\omega_p\omega_{h1}\omega_a}{(\omega_5-\omega_4)(\omega_1-\omega_4)(\omega_2-\omega_4)(\omega_3-\omega_4)} \tag{42}$$

$$C_5 = \frac{(\omega_{h2}+\omega_{br}-\omega_5)\omega_p\omega_{h1}\omega_a}{(\omega_1-\omega_5)(\omega_2-\omega_5)(\omega_3-\omega_5)(\omega_4-\omega_5)} \tag{43}$$

$$D_4 = \frac{(\Omega_{h2}+\Omega_{br}-\Omega_4)\Omega_p\omega_{h1}\omega_a}{(\Omega_5-\Omega_4)(\omega_1-\Omega_4)(\omega_2-\Omega_4)(\omega_3-\Omega_4)} \tag{44}$$

$$D_5 = \frac{(\Omega_{h2}+\Omega_{br}-\Omega_5)\Omega_p\omega_{h1}\omega_a}{(\omega_1-\Omega_5)(\omega_2-\Omega_5)(\omega_3-\Omega_5)(\Omega_4-\Omega_5)} \tag{45}$$

[1] A. S. Spirin, *Ribosomes*, (Springer, 2000).
[2] A.S. Spirin, FEBS Lett. **514**, 2 (2002).
[3] A. S. Spirin, J. Biol. Chem. **284**, 211203 (2009).
[4] R. A. Cross, Nature **385**, 18 (1997).
[5] V. Ramakrishnan, Angew. Chem. Int. Ed. **49**, 4355 (2010).
[6] A. Yonath, Angew. Chem. Int. Ed. **49**, 4340 (2010).
[7] T. A. Steitz, Angew. Chem. Int. Ed. **49**, 4381 (2010).
[8] T. A. Steitz, Nat. Rev. Mol. Cell Biol. **9**, 242 (2008).
[9] T. M. Schmeing and V. Ramakrishnan, Nature **461**, 1234 (2009).
[10] V. Ramakrishnan, Cell **108**, 557 (2002).
[11] J. Frank and C.M.T. Spahn, Rep. Prog. Phys. **69**, 1383 (2006).
[12] K. Mitra and J. Frank, Annu. Rev. Biophys. Biomol. Struct. **35**, 299 (2006).
[13] X. Agirrezabala and J. Frank, Quart. Rev. Biophys. **42**, 159 (2009).
[14] J. Frank and R. L. Gonzales, Annu. Rev. Biochem. **79**, 381 (2010).
[15] R.A. Marshall, C.E. Aitken, M. Dorywalska and J.D. Puglisi, Annu. Rev. Biochem. **77**, 177 (2008).
[16] J.B. Munro, A. Vaiana, K.Y. Sanbonmatsu and S.C. Blanchard, Biopolymers **89**, 565 (2008).
[17] J. B. Munro, K. Y. Sanbonmatsu, C.M.T. Spahn and S.C. Blanchard, Trends in Biochem. Sci. **34**, 390 (2009).

[18] S.C. Blanchard, Curr. Opin. Struct. Biol. **19**, 103 (2009).
[19] S. Blanchard, R.L. Gonzalez Jr., H.D. Kim, S. Chu and J.D. Puglisi, Nat. Str. & Mol. Biol. **11**, 1008 (2004).
[20] S. Uemura, C. E. Aitken, B.A. Flusberg, S. W. Turner and J.D. Puglisi, Nature **464**, 1012 (2010).
[21] C. E. Aitken and J. D. Puglisi, Nat. Struct. Mol. Biol. **17**, 793 (2010).
[22] J. R. Buchan and I. Stansfield, Biol. Cell **99**, 475-487 (2007).
[23] J.D. Wen, L. Lancaster, C. Hodges, A.C. Zeri, S.H. Yoshimura, H.F. Noller, C. Bustamante and I. Tinoco Jr., Nature **452**, 598 (2008).
[24] I. Tinoco Jr. and J. D. Wen, Phys. Biol. **6**, 025006 (2009).
[25] A. Garai, D. Chowdhury, D. Chowdhury and T. V. Ramakrishnan, Phys. Rev. E **80**, 011908 (2009).
[26] A. Basu and D. Chowdhury, Phys. Rev. E **75**, 021902 (2007).
[27] A. K. Sharma and D. Chowdhury, Phys. Rev. E **82**, 031912 (2010).
[28] M. Dixon and E.C. Webb, *Enzymes* (Academic Press, 1979).
[29] C. MacDonald, J. Gibbs and A. Pipkin, Biopolymers, **6**, 1 (1968).
[30] C. MacDonald and J. Gibbs, Biopolymers, **7**, 707 (1969).
[31] G. Lakatos and T. Chou, J. Phys. A **36**, 2027 (2003).
[32] L.B. Shaw, R.K.P. Zia and K.H. Lee, Phys. Rev. E **68**, 021910 (2003).
[33] L.B. Shaw, J.P. Sethna and K.H. Lee, Phys. Rev. E **70**, 021901 (2004).
[34] L.B. Shaw, A.B. Kolomeisky and K.H. Lee, J. Phys. A **37**, 2105 (2004).
[35] T. Chou, Biophys. J., **85**, 755 (2003).
[36] T. Chou and G. Lakatos, Phys. Rev. Lett. **93**, 198101 (2004).
[37] J.J. Dong, B. Schmittmann and R.K.P. Zia, J. Stat. Phys. **128**, 21 (2006).
[38] J.J. Dong, B. Schmittmann and R.K.P. Zia, Phys. Rev. E **76**, 051113 (2007).
[39] L. J. Cook, R. K. P. Zia and B. Schmittmann, Phys. Rev. E **80**, 031142 (2009).
[40] L. Ciandrini, I. Stansfield and M. C. Romano, Phys. Rev. E **81**, 051904 (2010).
[41] N. Mitarai, K. Sneppen and S. Pedersen, J. Mol. Biol. **382**, 236 (2008).
[42] M. V. Rodnina and W. Wintermeyer, Annu. Rev. Biochem. **70**, 415 (2001).
[43] T. Daviter, K. B. Gromadski and M. V. Rodnina, Biochimie **88**, 1001 (2006).
[44] J. M. Ogle and V. Ramakrishnan, Annu. Rev. Biochem. **74**, 129 (2005).
[45] H. S. Zaher and R. Green, Cell **136**, 746 (2009).
[46] D. Moazed and H. F. Noller, Nature **342**, 142 (1989).
[47] K. S. Wilson and H. F. Noller, Cell **92**, 337 (1998).
[48] H. F. Noller, FEBS Lett. **514**, 11 (2002).
[49] L. H. Horan and H. F. Noller, PNAS **104**, 4881 (2007).
[50] A. Korostelev, D. N. Ermolenko and H. F. Noller, Curr. Opin. Chem. Biol. **12**, 674 (2008).
[51] J. Frank and R. K. Agrawal, Nature **406**, 318 (2000).
[52] M. Valle, A. Zavialov, J. Sengupta, U. Rawat, M. Ehrenberg and J. Frank, Cell **114**, 123 (2003).
[53] J. Frank, H. Gao, J. Sengupta, N. Gao and D. J. Taylor, PNAS **104**, 19671 (2007).
[54] D. Pan, S.V. Kirillov and B.S. Cooperman, Mol. Cell **25**, 519 (2007).
[55] S.J. Moran, J. F. Flanagan, O. Namy, D.I. Stuart, I. Brierley and R.J.C. Gilbert, Structure **16**, 664 (2008).
[56] S. Shoji, S. E. Walker and K. Fredrick, ACS Chem. Biol. **4**, 93 (2009).
[57] M.E. Fisher and A.B. Kolomeisky, PNAS **96**, 6597 (1999).
[58] M.E. Fisher and A.B. Kolomeisky, Annu. Rev. Phys. Chem. **58**, 675 (2007).
[59] T. L. Hill, *Free energy transduction and biochemical cycle kinetics* (Dover, 2005).
[60] Y.R. Chemla, J.R. Moffitt and C. Bustamante, J. Phys. Chem. B **112**, 6025 (2008).
[61] J.W. Shaevitz, S.M. Block and M.J. Schnitzer, Biophys. J. **89**, 2277 (2005).
[62] J.C. Liao, J.A. Spudich, D. Parker, S.L. Delp, PNAS **104**, 3171 (2007).
[63] M. Linden and M. Wallin, Biophys. J. **92**, 3804 (2007).
[64] D. Tsygankov, M. Lindén, and M. E. Fisher, Phys. Rev. E **75**, 021909 (2007).
[65] A. Garai and D. Chowdhury, Submitted for publication.
[66] S. Redner, *A Guide to First-Passage Processes*, (Cambridge University Press, 2001).
[67] H. Qian and E.L. Elson, Biophys. Chem. **101-102**, 565 (2002).
[68] B.P. English, W. min, A.M. van Oijen, K.T. Lee, G. Luo, H. Sun, B.J. Cherayil, S.C. Kou and X.S. Xie, Nat. Chem. Biol. **2**, 87 (2006).
[69] S.C. Kou, B.J. Cherayil, W. Min, B.P. English and X.S. Xie, J. Phys. Chem. B **109**, 19068 (2005).
[70] W. Min, B.P. English, G. Luo, B.J. Cherayil, S.C. Kou and X. S. Xie, Acc. Chem. Res. **38**, 923 (2005).
[71] W. Min, I.V. Gopich, B.P. English, S.C. Kou, X.S. Xie and A. Szabo, J. Phys. Chem. B **110**, 20093-20097 (2006).
[72] M. Basu and P.K. Mohanty, arxiv.0901.2844 (2009).
[73] J. J. Hopfield, T. Yamane, V. Yue and S.M. Coutts, Proc. Nat. Acad. Sci. USA **73**, 1164 (1976).
[74] T. Yamane and J. J. Hopfield, Proc. Nat. Acad. Sci. USA **74**, 2246 (1977).
[75] Y. Arava, Y. Wang, J.D. Storey, C.L. Liu, P.O. Brown and D. Herschlag, PNAS **100**, 3889 (2003).
[76] P J. Farabaugh, Prog. Nucl. Acid Res. Mol. Biol. **64**, 131 (2000).